

CSR SHIELDING EXPERIMENT*

V.Yakimenko[#], M.Fedurin, V.N. Litvinenko A.V. Fedotov, D.Kayran, BNL, Upton, NY
P. Muggli, USC, Los Angeles, CA

Abstract

It is well known that the emission of coherent synchrotron radiation (CSR) in a dipole magnets leads to increase in beam energy spread and emittance. At the Brookhaven National Laboratory Accelerator Test Facility (ATF) we study the suppression of CSR emission affect on electron beam in a dipole magnet by two vertically spaced conducting plates. The gap between the plates is controlled by four actuators and could be varied from 0 to 14 mm.

Our experimental results show that closing the plates significantly reduces both the beam energy loss and CSR-induced beam energy spread. In this paper we present selected results of the experiment and compare then with rigorous analytical theory.

INTRODUCTION

There are a number of publications investigating the self-effect of CSR on a bunch energy spectrum. A comprehensive collection can be found in [1]. The possibility of using shielding plates to compensate this effect was suggested in [2]. Mean energy loss compensation was experimentally observed [3] and agrees well with predictions [4]. Authors are not aware of experimental results that report direct experimental observation of the shielding plates effect on the beam energy spread. Experimental observations and supporting theoretical estimates presented in this paper lead to different conclusion from previous work [5]: shielding plates can significantly reduce the energy spread increase induced on a bunch by CSR in a bending magnet.

DESCRIPTION OF EXPERIMENT

The experiment was carried out at Brookhaven Accelerator Test Facility. For optimized beam parameters, an energy spectrum change at the level of 10 keV was expected in a single pass through a dipole magnet. A beam energy stability at the level of $\delta E/E \sim 10^{-5}$ was needed to reliably characterize the effect. The high brightness electron beam was produced by a 1.6 cell photoinjector RF gun and then accelerated by a 6-m long S-band linac to 57.6MeV. Running the linac off crest induced a energy-time correlation on the beam. In the dispersive region of the transport line an energy selection collimator was used to select a ≈ 2 ps long bunch by allowing a 200keV slice of the original beam to pass. Very stable beam conditions were achieved as a result: a slightly different part of the original beam in time was selected due to natural shot to shot energy jitter, yet the

selected beam ended up with the same energy spectrum. The slow feedback system that stabilizes the beam energy at the 10^{-4} level and the RF phase at the 0.25 degree level was utilized.

The method is very similar to the mask technique that was developed and actively used for different experiments at ATF and described in more details in [6]. Large ratio of horizontal dispersion to the beta functions at energy collimator location (~ 12.5 m in figure 1), low emittance and local energy spread allow for the generation of a flat top pulse with sharp rise and fall in times. The linear energy time correlation of the selected beam was utilized to measure the beam time by analyzing beam images on the energy spectrometer.

Aluminum shielding plates were installed in the second dipole ($s=20$ m on Fig. 1). The material polished to the submicron level of flatness was used to reduce influence of surface roughness wake-fields. A 0.4-meter long dipole magnet with a 20-degree bending angle was used for the experiment. The plates expand 0.15 cm on each side of the dipole to cover the edge field regions for a total length of 0.7 m. The beam was drastically shortened in the dispersive region of the beam line, after the first dipole. As a result, the CSR effect is much stronger in the second dipole and shielding plates were not installed in the first dipole.

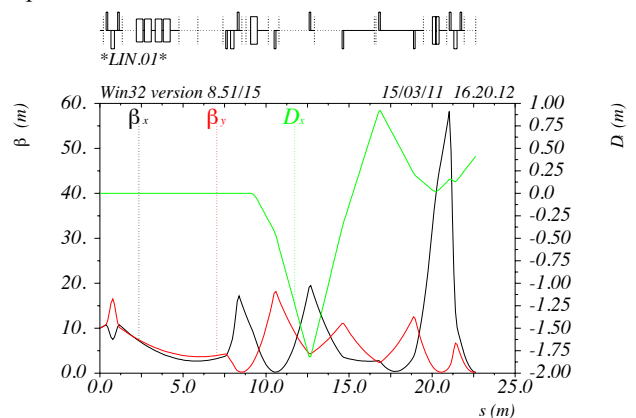


Figure 1: Optical function of the transport line from the linac exit to the spectrometer beam profile monitor. The energy collimator is located at position of 12.5 m and the magnet with shielding plates at the 20 m position.

Beam Twiss parameters starting from the linac exit and to the energy spectrometer are shown in Figure 1. The focusing was design to have a zero dispersion function in the center of the magnet with the shielding plates in order to minimize the influence of transverse effects. Small vertical beta function in combination with low emittance were essential for loss-free transmission of the beam through the 0.7 m long shielding plates closed down to a

*Work supported by supported by Brookhaven Science Associates, LLC under Contract No. DE-AC02-98CH10886 with the U.S. Department of Energy

[#]yakimenko@bnl.gov

minimum gap of 1 mm. The large number of beam profile monitors available along the transport line allowed for experimentally verifying the optical functions to better than 10% accuracy.

MEASUREMENTS

The selected beam duration was measured using autocorrelation of the Coherent Transition Radiation signal generated by the beam from a copper mirror. A liquid helium cooled bolometer in combination with a Michelson interferometer yielded traces similar to that shown in Figure 2.

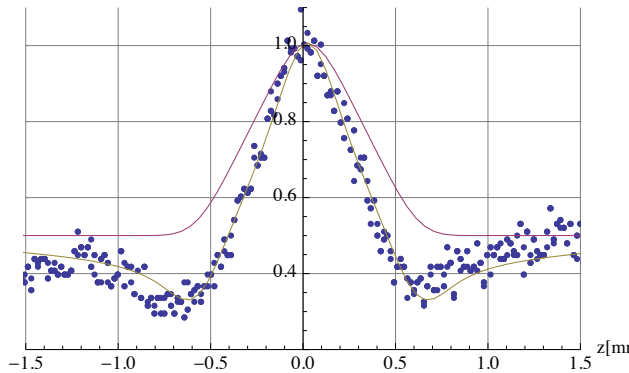


Figure 2: Measured CTR autocorrelation trace of the electron beam (points). Calculated autocorrelation trace of the flat-top 600micron long (FWHM) pulse with 50 microns rise/fall is shown (violet line). Autocorrelation trace calculated with low frequency cut-off mimicking that of the detection system (brown line).

As shown in Fig. 1, the beam was tightly focused on the Beam Profile monitor with the triplet following the second dipole with the CSR-suppression plates. High-resolution energy spectrum images were obtained as a result. A combination of the images that show energy spectrum change for different plate gap position is shown in Fig. 3.

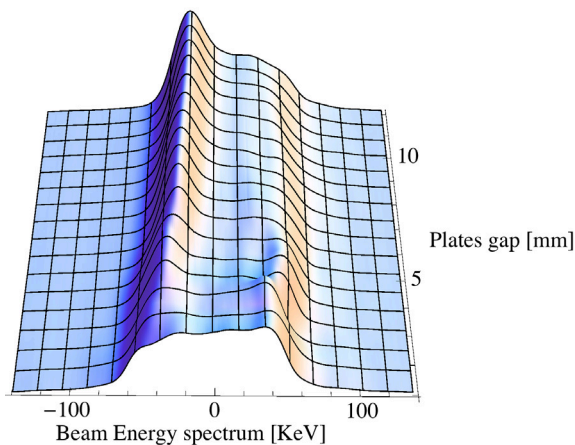


Figure 3: Measured beam energy spectrum as function of the gap between the shielding plates.

The energy correlation on the beam was selected such that the head of the beam has a lower energy, while the tail of the beam has a higher energy. One can clearly observe that for larger plate opening, particles in the head of the beam (lowest energy particles) gain energy and move towards the middle of the distribution. Similarly particles in the tail (highest energy particles) loose energy and also move toward the middle of the distribution. This energy exchange is not observable at the plate gap of 3 mm and lower. These effects are even more visible on Fig. 4 that plots the difference between the energy spectra with various plate openings and that for an opening of 1mm (CSR effect suppressed).

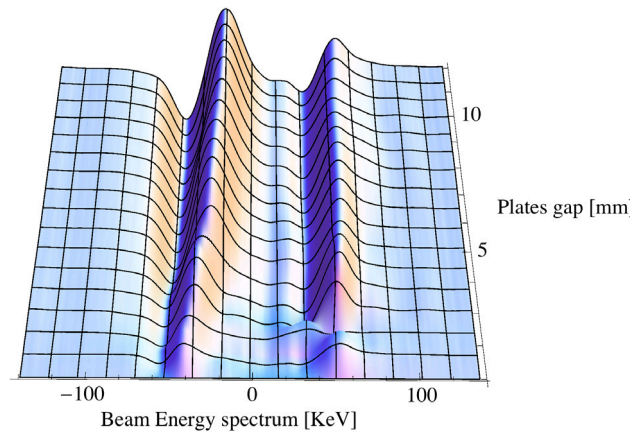


Figure 4: Charge displacement map calculated from results shown in Fig. 3.

ANALYTICAL FORMULAE

The simple geometry of two parallel conducting plates allows for the derivation of an exact analytical expression for the CSR wake-field for an arbitrary longitudinal bunch profile described by the following normalized distribution: $f(\varphi)$; $\varphi = (s - s_o)/R_o$, where $R_o = 1.14$ m is the radius of the electron's trajectory curvature in the bending magnet.

Using classical expressions for the retarded radiated field [7], one can express the total longitudinal CSR wake-field as:

$$W(\varphi) = \frac{2e\beta^2}{R_o^2} N_e \sum_{n=-\infty}^{\infty} (-1)^n \cdot \int_{-\infty}^{\infty} d\psi \cdot f(\varphi - 2\psi + \beta\rho_n(\psi)) \cdot \left(1 - \beta \frac{\sin 2\psi}{\rho_n(\psi)} \right) \cdot \frac{(-\rho_n^2(\psi) \sin 2\psi + 2 \sin^2 \psi \rho_n(\psi) \beta + 4 \cos \psi \sin^3 \psi)}{(\rho_n(\psi) - \beta \sin 2\psi)^3} \quad (1)$$

using for parameterization the retarded angle $\psi = (\theta_t(t) - \theta_n(t'))/2$ (with $\theta_t(t)$ being the angular position of the test particle at moment t and $\theta_n(t')$ being

the angular position of the radiating particle at retarded time t') [8]. The expression

$$\rho_n(\psi) = \sqrt{4 \sin^2 \psi + n^2 h^2 / R_o^2} \quad (2)$$

in eq. (1) is nothing else than the dimensionless distance between the radiation and the observation point, where n is the image number of the reflection in the plates and h is the full gap between the plates.

Detailed description of the derivation and the analysis of the shielded CSR wake-fields will be published elsewhere [9]. In this short paper we show only few selected results. First, Fig. 5 and 6 show the calculated CSR wake-fields using the analytical formula (1) and the e-beam profile described in Fig.2.

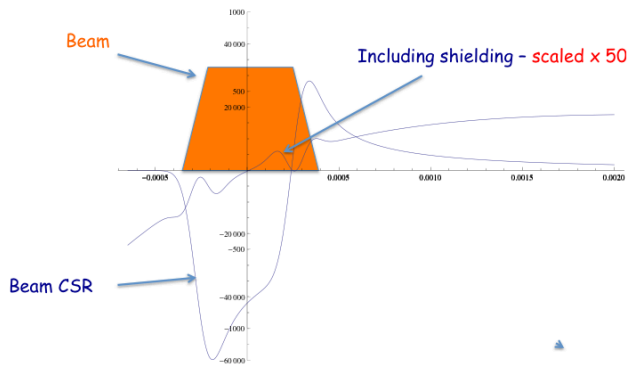


Figure 5: Calculated CSR wake-fields for the unshielded and shielded case with 1 mm gap. For visibility the CSR wake-field for 1 mm gap is multiplied by 500. The horizontal scale is φ in radians.

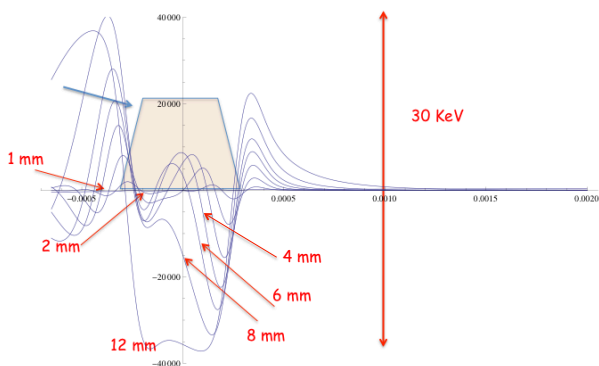


Figure 6: CSR wake-field as the function of the gap between the plates. The vertical scale is 0.38 eV per unit, the horizontal scale is φ in radians.

The value of the wake-field sensed by the beam itself is of most practical importance since it affects both the energy loss and the induced energy spread. We call the variation of wake-field sensed by the e-beam as the span of the wake-field.

It is absolutely clear from these direct calculations that a small gap reduces both the energy loss and the CSR-induced energy spread. To be exact, closing the gap from 12 mm to 1mm reduces the span of CSR wake-field affecting the beam from 30 KeV to 190 eV, i.e. a 160-folds reduction.

Beam Dynamics and EM Fields

Dynamics 04: Instabilities

The results of our analytical studies are in good qualitative agreement with the measurements. For example, both the exact analytical theory and the experiment show that effective suppression of the CSR wake-field span happens only at very small gaps ~ 1 mm. Opening the gap from 1 mm to 2 mm, increases the CSR wake-field span 4-folds. At a 4 mm gap, the span is almost identical to that of unshielded wake, even though it has more oscillations (i.e. less net loss) than the unshielded wake. It is also quite clear that plates with 12 mm gap affect only long-range wings of the wake-field, i.e. almost do not change the CSR effect on the beam.

Fig. 7 shows results of preliminary simulations of the modification of the e-beam energy spectrum for four selected gaps: 1, 2, 8 and 12 mm. Again, qualitatively the spectrum modifications are in agreement with the measurements.

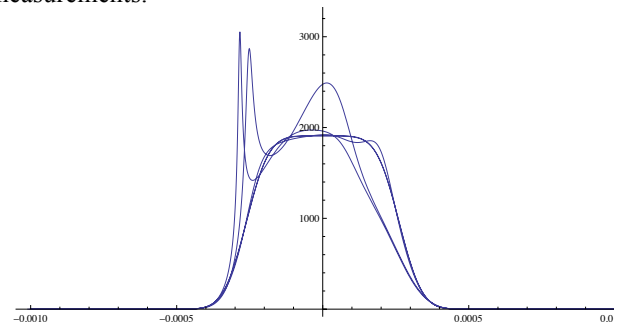


Figure 7: Simulations of the beam energy spectrum dependence on the gap between the plates: the two distributions with “horns” are for 12 and 8 mm gaps. The two others are for 1 and 2 mm gaps.

CONCLUSIONS

We presented clear experimental observation of suppression of the longitudinal CSR wake in a dipole magnet by two conducting plates. At very small gaps we observed the suppression of both the energy loss and the energy spread induced by CSR. Our analytical results are in good agreement with observations.

REFERENCES

- [1] J.Murphy, ICFA Beam Dynamics Newsletter No. 35 (2004)
- [2] L. I. Schiff, Rev. Sci. Instrum. 17, 6 (1946)
- [3] R. Kato et.al, Phys. Rev. E 57, 3454–3460 (1998)
- [4] J. S. Nodvick et.al, Phys. Rev. 96, 180 (1954)
- [5] C. Mayers and G. Hoffstaetter, PRST/AB 12, 024401 (2009)
- [6] P. Muggli, et.al. Phys. Rev. Lett. 101, 054801 (2008)
- [7] L.D. Landau and E.M. Lifshitz, “The Classical Theory of Fields”, Pergamon Press, Fourth Edition, 1975, p. 162, formula (63.8)
- [8] V.N.Litvinenko, CSR, Duke FEL Lab Notes, 1998
- [9] in preparation